Optimization of TiO_2/Cu/TiO_2 multilayers as a transparent composite electrode deposited by electron-beam evaporation at room temperature*

Sun Hong-Tao(孙洪涛), Wang Xiao-Ping(王小平)†, Kou Zhi-Qi(寇志起), Wang Li-Jun(王丽军), Wang Jin-Ye(王金烨), and Sun Yi-Qing(孙义清)

College of Science, University of Shanghai for Science and Technology, Shanghai 200093, *China*

(Received 27 July 2014; revised manuscript received 28 October 2014; published online 10 February 2015)

Highly transparent indium-free composite electrodes of TiO_2/Cu/TiO_2 are deposited by electron-beam evaporation at room temperature. The effects of Cu thickness and annealing temperature on the electrical and optical properties of the multilayer film are investigated. The critical thickness of Cu mid-layer to form a continuous conducting layer is found to be 11 nm. The multilayer with a mid-Cu thickness of 11 nm is optimized to obtain a resistivity of 7.4×10^{-5} Ω·cm and an average optical transmittance of 86% in the visible spectral range. The figure of merit of the TiO_2/Cu(11 nm)/TiO_2 multilayer annealed at 150 °C reaches a minimum resistivity of 5.9×10^{-5} Ω·cm and an average optical transmittance of 88% in the visible spectral range. The experimental results indicate that TiO_2/Cu/TiO_2 multilayers can be used as a transparent electrode for solar cell and other display applications.

Keywords: multilayer, transparent conductor, thin film, annealing

PACS: 77.55.–g, 68.55.–a, 81.15.Hi **DOI:** 10.1088/1674-1056/24/4/047701

1. Introduction

Transparent conducting oxide (TCO) thin film exhibits high electrical conductivity as well as high transparency in the visible solar spectrum and high reflectivity in the infrared region. TCOs are widely used in opto-electronic devices, such as solar cells, panel displays, electrochromic devices, liquid crystal displays, etc.[1–6] Indium tin oxide (ITO) with a high transmittance of ∼ 80% and a low electrical resistance of $\sim10^{-5}$ Ω·cm is currently used as a transparent conducting electrode. However, indium is rare and toxic, which restricts its applications. Thus, it is of significance to search for cheaper materials with good opto-electrical properties. Contending indium-free transparent conductors include indium-free transparent conductive oxides, graphene films, and carbon nanotubes.[7] Recently, multilayer coatings of the oxide/metal/oxide (OMO) have been investigated to develop a transparent composite electrode with the desired electrical conductivity.[8–12] In comparison, the OMO multilayer has low sheet resistance and high transparence. The addition of a thin metal layer in the middle will reduce the effective resistivity of the multilayer without much loss in optical transmittance. The top dielectric layer can suppress the reflection from the metal layer and obtain a higher transparent effect.

Titanium dioxide (TiO_2) is a potential semiconductor material with a wide band gap (∼ 3 eV). It has a lot of excellent physical properties such as a high dielectric constant, a strong mechanical stability, and a strong chemical stability.[13] TiO_2 oxide material is selected to be used in the OMO structure due to its high refractive index of 2.7 and excellent optical transparency of above 90% in the visible region. The top TiO_2 layer also protects the metal from deteriorating the properties during exposure to some environmental conditions. As is well known, the sandwich structure films of TiO_2/Ag/TiO_2 have achieved excellent results because of the high conductivity of Ag.[14] Though metallic Ag has a very low resistivity, Ag is expensive and easy to oxidize. So it still needs to be improved in some aspects such as the selection of another intermediate metal layer. Metal copper (Cu) has a much lower cost, better oxidation resistance, and comparable resistivity (approximately 1.7×10^{-6} Ω·cm) to the Ag resistivity (approximately 1.6×10^{-6} Ω·cm). It should be more valuable for actual applications. To date, there have been fewer reports related to Cu serving as the intermediate layers in TiO_2-based sandwich structures.

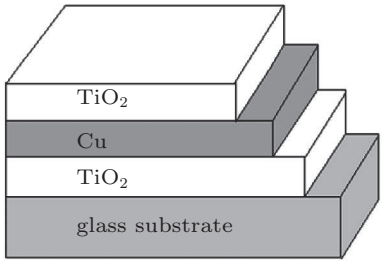


Fig. 1. Layered structure of TiO_2/Cu/TiO_2 multilayer film.

*Project supported by the Research Innovation Key Project of Education Committee of Shanghai, China (Grant No. 14ZZ137) and the National Cultivation Fund from University of Shanghai for Science and Technology (Grant No. 14XPM04).

†Corresponding author. E-mail: wxpchina64@aliyun.com, wxpchina@sohu.com

© 2015 Chinese Physical Society and IOP Publishing Ltd

In this work, metal Cu is chosen as the interlayer metal. TiO_2/Cu/TiO_2 (TCT) transparent conductive electrodes are prepared by electron beam vapor deposition (EBVD) apparatus at room temperature. The influences of Cu thickness and annealing temperature on photoelectric properties of TCT multilayer electrodes are investigated. The sandwiched structure of TiO_2/Cu/TiO_2 multilayer film is shown in Fig. 1.

2. Experiment

Multilayer films of TCT of different Cu thickness values were sequentially deposited on 1.2-mm-thick glass at room temperature using a titanium oxide (99.9995% purity) and metal Cu targets (99.999% purity) in an electron beam evaporation deposition system. The glass substrates were ultrasonically cleaned in acetone, absolute ethyl alcohol, and dried in flowing nitrogen gas before deposition subsequently. A mechanical pump coupled with a molecular pump was utilized to achieve 2.7×10^{-3} Pa before introducing oxygen gas (99.9995% purity). Details of the deposition procedure are described in Table 1. The thickness values of the bottom-layer and top-layer of TiO_2 were both about 20 nm, and the thickness of the Cu layer was varied between 8 nm and 15 nm. After the deposition process, the TiO_2/Cu (11 nm)/TiO_2 thin film was annealed at diverse temperatures in air for 0.5 hour.

The surface roughness was determined and a surface image is taken by field emission scanning electron microscope (FE-SEM); the crystal orientation of the film was investigated by x-ray diffraction (XRD); the sheet resistance (R_S) was measured using the four-point probe method; carrier concentration was measured by a Hall effect measurement system; optical transmittance was measured in a range of 300 nm–800 nm by an ocean optics double channel spectrometer (model Lambda-1050).

Table 1. Technological parameters of TiO_2/Cu/TiO_2 multilayer films fabricated by EBVD.

	Top and bottom TiO_2 layer	Cu mid-layer
Beam current/mA	60	80
Substrate temperature/°C	30	30
Oxygen gas flow/sccm	5	0
Thickness/nm	20	8–15
Voltage/kV	6	8
Filament current/A	0.5	0.8
Not coating vacuum/Pa	5.7×10^{-3}	3×10^{-3}
Coating vacuum/Pa	1.2×10^{-2}	5.8×10^{-3}

3. Results and discussion

3.1. Influence of Cu thickness on photoelectric properties of TiO_2/Cu/TiO_2 multilayer film

Figure 2 shows optical transmittance spectra in a wavelength range of 300 nm–800 nm for multilayer films with different thickness values of Cu layers. The maximum optical transmittance of the pure single-layer TiO_2 film is about 90% in the visible region. Although metal Cu has a high reflectivity, very thin films ($<$ 15 nm) show moderate transmittances in the visible region and the top dielectric layer helps to obtain a higher transparent effect by diminishing the reflection from the metal layer.[15] As seen in Fig. 2, the optical transmittance of the multilayers increases as the Cu layer thickness increases from 8 nm to 11 nm. At a Cu thickness of 11 nm, the highest average transmittance of 86% in the visible spectral range is observed; this can be attributed to the evolution of the Cu layer, since Cu film with a thickness of less than 11 nm will have an island-shaped discontinuous micro-structure. The optical transmittance properties of the films can be understood in terms of the change in complex dielectric function for copper. In a discontinuous Cu film, a size-dependent variation in the dielectric function is known to exist due to the limitation of the mean free path of the conduction electrons. This leads to a correction to the imaginary part of the overall dielectric function (ε_R) given by[16]

$$\varepsilon_R = \varepsilon_m + \frac{C}{R}, \tag{1}$$

where ε_m is the dielectric constant of the bulk metal, C is a constant at a particular wavelength, and R is the particle radius. As a consequence, below the critical thickness, as the radius of the Cu island decreases, the transmittance decreases. As Cu thickness increases, the Cu becomes a continuous layer from discontinuous islands, which causes a decrease in light scattering. However, further increasing Cu thickness above 11 nm results in an abrupt decrease in transmittance from $\sim$ 86% to 73% for 15-nm-thick Cu layer due to the increase in plasmon absorption and reflectivity of the mid-Cu layer, although we note that the augment of Cu layer thickness can increase the effective resistivity of the multilayer film. Thus, the appropriate thickness of the Cu layer is necessary for achieving maximum transmittance. It is found that the optimum value of Cu layer thickness is 11 nm with an average transmittance of 86% in the visible spectral range.

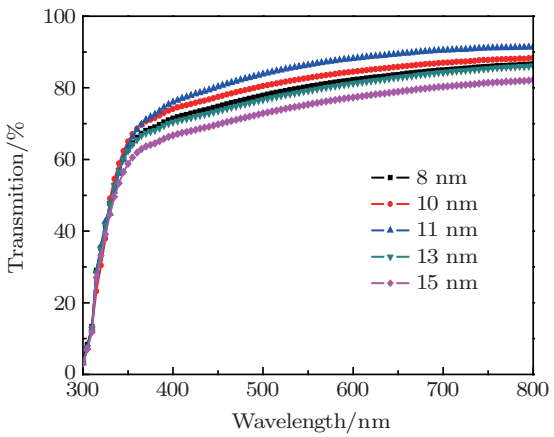


Fig. 2. (color online) Transmittance spectra of TCT multilayer films with different values of Cu interlayer thickness.

Figure 3 shows a parallel resistance circuit model of TCT multilayer film. The thickness of the Cu layer varies from 8 nm to 15 nm. The total resistance of the multilayer is a combination of the resistances of three consecutive layers, connected in parallel, and expressed as follows:[17]

$$\frac{1}{R} = \frac{1}{R_{\mathrm{TiO_2(Bottom)}}} + \frac{1}{R_{\mathrm{Cu}}} + \frac{1}{R_{\mathrm{TiO_2(Upper)}}}. \tag{2}$$

The value of R_{Cu} is much less than TiO_2 resistance, so the total resistance $R \approx R_{\mathrm{Cu}}$ and the total resistance depends mainly on the Cu layer. We know that a thin Cu film growing on a crystalline bottom layer follows the Stranski–Krastanov[18,19] growth mechanism of a layer plus-island growth model while Cu film growing on an amorphous TiO_2 surface should follow the island growth mechanism of the Volmer–Weber model.[19] On the basis of island growth, we expect the different conduction mechanisms[20] before and after the critical thickness of the Cu middle layer. It has been proposed that in the case of continuous Cu film, when the islands are connected, there will only be metal conduction; however, in the case of discontinuous metal film with islands, there will be a different resistance model which includes: metal conduction, dielectric conduction, and quantum tunneling. Here, the surface coverage of the discontinuous Cu thin film will take a predominant role in the conduction among dielectrics (metal oxides) or quantum tunnelings.

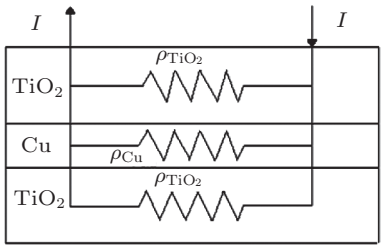


Fig. 3. Schematic diagram of parallel resistors in TCT multilayer film.

The four-point probe method is used for sheet resistance measurements. By using the four-point probe method, the semiconductor sheet resistance can be calculated from the following equation

$$R_{\mathrm{S}} = \frac{\pi}{\ln 2}\frac{V}{I}, \tag{3}$$

where V is the voltage reading on the voltmeter, I is the current carried by the two current-carrying probes. The sheet resistance is defined by $R_{\mathrm{S}} = \rho/d$, where ρ is the resistivity in Ω·cm and d is the coating thickness in cm. Figure 4 indicates the sheet resistance and resistivity of TCT multilayer film depending upon the thickness of the Cu layer. TiO_2 is an insulator with a resistivity on the order of 10^7 Ω·cm. On depositing an 8-nm Cu film between the TiO_2 layers, the resistivity decreases to 3.2×10^{-4} Ω·cm which suggests that there is an 11-fold decrease in resistivity in the TCT multilayer when compared with that in bare TiO_2. As the effective Cu thickness increases from 8 nm to 15 nm, the multilayer resistivity decreases gradually down to 4.9×10^{-4} Ω·cm. As seen in Fig. 4, the resistivity of TCT multilayers drops rapidly from 8 nm to 11 nm, because the Cu film with a thickness of less than 11 nm has an island-shaped discontinuous micro-structure, which is not well conductive. As the islands grow, the separation between the islands decreases and some of the islands coalesce to form a continuous layer. This leads to a radical drop in resistance. However, as the Cu layer thickness further increases above 11 nm, the effective resistivity of the multilayer with the TCT multilayer gradually decreases and approaches to the resistivity of bulk Cu. The change in effective resistivity of the TCT multilayer film with increasing the Cu thickness can be explained by the following basic relationship:[21]

$$\rho = \frac{1}{ne\mu}, \tag{4}$$

where ρ is the resistivity, n is the number of charge carriers, e is the charge of the carrier, and μ is the mobility. From this equation, we see that changes in mobility and carrier concentration can both affect the resistivity. When the Cu islands form a contiguous layer, the decrease in resistivity is governed by the combined effect of the increase in carrier concentration of conducting electrons and mobility.[22]

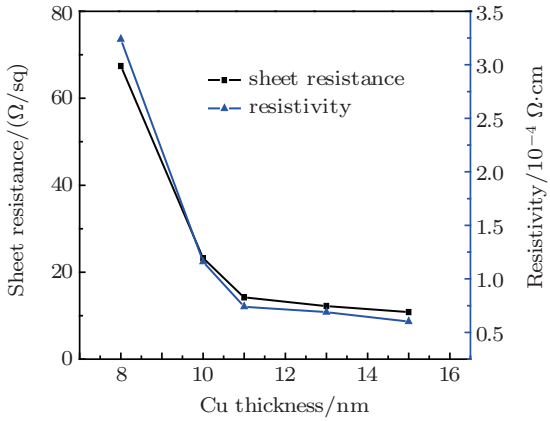


Fig. 4. (color online) Effects of Cu layer thickness on sheet resistance and resistivity of TCT multilayer film.

Figure 5 shows the change in carrier concentration with Cu thickness for TCT multilayer film. The plot indicates that the carrier concentration depends strongly on Cu thickness. The carrier concentration of the TCT multilayer films increases from 2.7×10^{21} cm^{-3} to 9.2×10^{21} cm^{-3} as effective Cu thickness increases from 8 nm to 15 nm. Hence, metallic conduction is dominant in this TCT system. There are many scattering mechanisms which can affect the mobility of carriers, and hence the resistivity of the film. Given that the conduction in the multilayer is primarily through the Cu mid-layer, the main scattering mechanisms that can influence charge carriers are interface scattering, surface scattering, or grain-boundary scattering.

A figure of merit, (as defined by Haacke) is estimated for each of the TCT multilayers using the following relationship

$$\varphi_{\rm TC} = \frac{T_{\rm av}^{10}}{R_{\rm sh}}, \tag{5}$$

where $T_{\rm av}$ is the transmittance and $R_{\rm sh}$ is the sheet resistance. The multilayer with a mid-Cu thickness of 11 nm (T: 86% and $R_{\rm sh}$: 14.2 Ω/sq) has a maximum figure of merit of 15.6×10^{-3} Ω^{-1}.

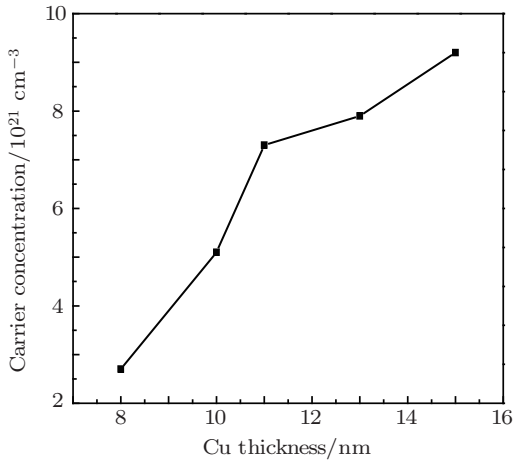


Fig. 5. Carrier concentrations of TCT multilayer film as a function of Cu thickness.

3.2. Influence of annealing temperature on photoelectric properties of TiO_2/Cu/TiO_2 multilayer film

In order to examine the thermal stabilities of the properties of multilayer films, TiO_2/Cu(11 nm)/TiO_2 multilayers are annealed at different temperatures (150 °C ∼400 °C) in air. Figure 6 shows the SEM morphological images of TiO_2/Cu(11 nm)/TiO_2 multilayer films annealed at different temperatures. As can be seen from the images, with increasing the annealing temperature, the grain size of TiO_2 increases and the uniformity is improved. Annealing treatment can change the surfaces of films more homogeneously with better coverage and reduction of the porosity of the films. This is consistent with the result of the crystalline properties. At high temperature, the atoms have enough diffuse activation energy to occupy the correct site in the crystal lattice and grains with the lower surface energy will become larger at high temperature.[23]

The crystalline structures of different multilayer films are determined by XRD measurements. Figure 7 shows the XRD patterns of the as-deposited TiO_2/Cu(11 nm)/TiO_2 multilayer films and post-deposition annealed films at different temperatures respectively. It is seen that in each XRD pattern there exists only the Cu (111) peak, but no apparent titanium dioxide crystalline peaks appear. As-deposited TiO_2/Cu (11 nm)/TiO_2 films do not show any strong diffraction peaks in the XRD patterns; this is due to the low substrate temperature and film being too thin to form a crystalline phase. Upon increasing the annealing temperature to 150 °C, the TiO_2/Cu(11 nm)/TiO_2 multilayer starts to show a crystalline Cu (111) peak at 43.3°. The intensity of the Cu (111) peak increases with annealing temperature rising. This finding can be understood based on the fact that the thermal energy during annealing may enable atoms to diffuse and stack. As a result, the number of deposition defects is reduced and a more perfect crystal structure is formed.[24]

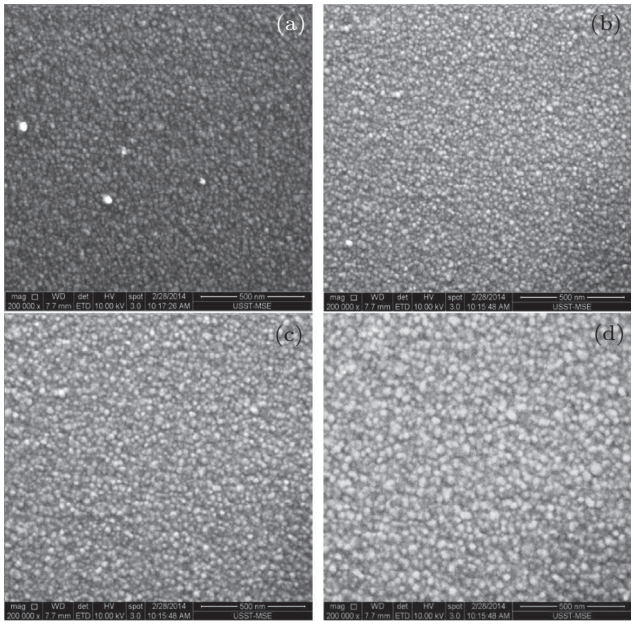


Fig. 6. SEM micrographs of TiO_2/Cu(11 nm)/TiO_2 multilayer films annealed at various temperatures: (a) as-deposited, (b) 150 °C, (c) 250 °C, (d) 350 °C.

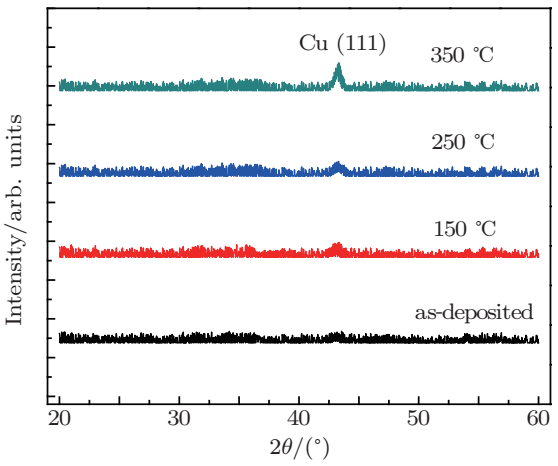


Fig. 7. (color online) The x-ray diffraction patterns of TiO_2/Cu(11 nm)/TiO_2 multilayer films annealed at various temperatures.

Figure 8 indicates the effects of annealing on the sheet resistance and resistivity of the TiO_2/Cu(11 nm)/TiO_2 multilayer film. The resistivity of the as-deposit film is 7.4×10^{-5} Ω·cm. It decreases slightly with temperature until 150 °C, where the resistivity has a highest value of 5.9×10^{-5} Ω·cm, which is

attributed to the improved crystal quality of TiO_2 film and efficient protection from forming Cu-oxide.[25] However, with further increase of annealing temperature, the sheet resistance increases, and the resistivity of the TiO_2/Cu(11 nm)/TiO_2 multilayer increases drastically to 1.51×10^{-4} Ω·cm at an annealing temperature of 350 °C. For such a deterioration, two primary reasons have been found: one is an agglomeration of Cu film during annealing, which leads to the sheet resistance increase by the enhanced surface scattering effect;[26] the other is that the effective thickness of the Cu layer becomes thinner. The Cu has a high diffusion coefficient and it can migrate quickly into the TiO_2 film in the heat process and the effective thickness of the Cu layer becomes thinner. Therefore, the resistivity increases as temperature further increases. While the annealing temperature is above 400 °C, the resistivity of the multilayer film becomes very high, almost as high as an insulator resistivity. This can be attributed to the oxidation of the Cu layer, when the heat treatment takes place in air, an oxygen atom in the air diffuses through the TiO_2 layer and oxidizes the Cu layer partly.

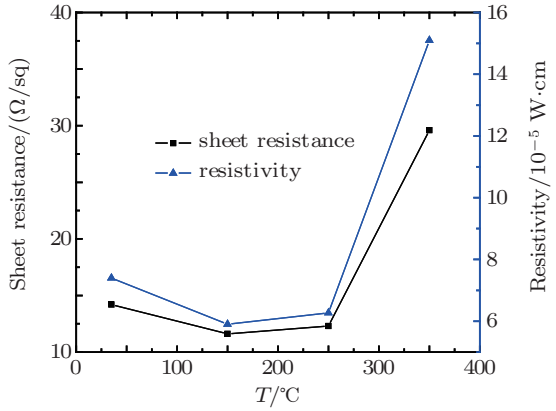


Fig. 8. (color online) Sheet resistance and resistivity of TiO_2/Cu(11 nm)/TiO_2 multilayer films annealed at various temperatures.

Figure 9 shows the effects of annealing on the transmittance of the TiO_2/Cu(11 nm)/TiO_2 multilayer films. It is observed that the optical transmittance increases with the increase of annealing temperature up to 150 °C. The TiO_2/Cu(11 nm)/TiO_2 multilayer with 150-°C annealing temperature shows a maximum average optical transmittance of around 88%. With the further increase of annealing temperature, multilayer performance decreases. This phenomenon can be explained as follows. Because of the better crystallization degree of TiO_2 (Fig. 6), there are fewer grain boundaries, which will reduce the scattering of incident light. As a result, the transmittance increases. However, with further increasing the annealing temperature, on the one hand, the surface roughening due to agglomeration of Cu film during annealing results in more scatterings of the incident light and decreasing of transmittance.[27] On the other hand, diffusion of Cu atoms onto the TiO_2 film by annealing may reduce the antireflection effect of the TiO_2 film due to the higher optical absorption of Cu atoms, resulting in lower optical transmittance.[28]

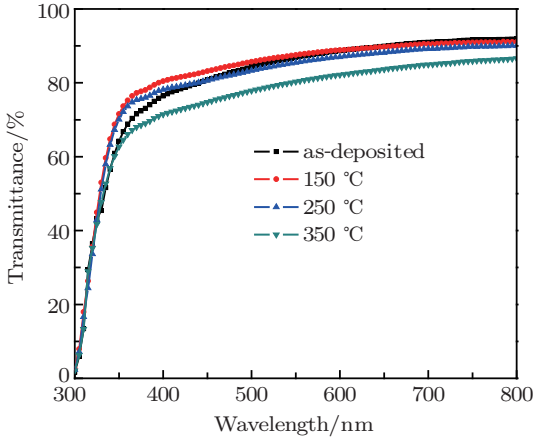


Fig. 9. (color online) Optical transmission spectra of TiO_2/Cu(11 nm)/TiO_2 multilayer films at various annealing temperatures.

4. Conclusions

A series of multilayer structures of TCT is successively prepared by the electron beam evaporation method at room temperature to prepare indium-free transparent composite electrodes. The Cu layer thickness has effects on the transmittance and the electrical properties of TCT multilayer. The multilayer with a mid-Cu thickness of 11 nm is optimized to have a resistivity of 7.4×10^{-5} Ω·cm and an average optical transmittance of above 86% in the visible spectral range. The effects of annealing temperature on the structural, optical, and electrical properties of the TCT films are also investigated. The figure of merit of the TiO_2/Cu(11 nm)/TiO_2 film annealed at 150 °C reaches a minimum resistivity of 5.9×10^{-5} Ω·cm and an average optical transmittance of above 88% in the visible spectral range. These experimental results suggest that TCT multilayers can be used as transparent electrodes for solar cell and other display applications.

References

[1] Look D C, Leedy K D, Tomich D H and Bayraktaroglu B 2010 *Appl. Phys. Lett.* **96** 062102
[2] Wan Q, Dattoli E N and Lu W 2007 *Appl. Phys. Lett.* **90** 222107
[3] Ishida T, Okada M, Tsuchiya T, Murakami T and Nakano M 2011 *Thin Solid Films* **519** 1934
[4] Gustafsson G, Cao Y, Treacy G M, Klavetter F, Colaneri N and Heeger A J 1992 *Nature* **357** 477
[5] Zhang W W, Liu F M, Cai L G, Zhou C C, Ding P and Zhang H A 2010 *Chin. Phys. B* **19** 107306
[6] Chen Y Y, Wang X, Cai X K, Yuan Z J, Zhu X M, Qiu D J and Wu H Z 2014 *Chin. Phys. B* **23** 026101
[7] Kumar A and Zhou C 2010 *ACS Nano* **4** 11
[8] Indluru A and Alford T L 2009 *J. Appl. Phys.* **105** 123528
[9] Park T Y, Choi Y S, Kang J W, Jeong J H, Park S J, Jeon D M, Jeon J W and Kim Y C 2010 *Appl. Phys. Lett.* **96** 051124

[10] Daeil K 2012 *Opt. Commun.* **285** 1212
[11] Ghosh D S, Chen T L and Pruner V 2010 *Appl. Phys. Lett.* **96** 041109
[12] Lee J H, Woo K Y, Kim K H, Kim H D and Kim T G 2013 *Opt. Lett.* **38** 5055
[13] Hashimoto K, Irie H and Fujhishima A 2005 *Jpn. J. Appl. Phys.* **44** 8269
[14] Dhar A and Alford T L 2013 *APL Materials* **1** 012102
[15] Liu X, Cai X, Qiao J, Mao J and Jiang N 2003 *Thin Solid Films* **44** 200
[16] Sivaramakrishnan K and Alford T L 2010 *Appl. Phys. Lett.* **96** 201109
[17] Ryu S Y, Noh J H, Hwang B H, Kim C S, Jo S J, Kim J T, Hwang H S, Baik H K, Jeong H S, Lee C H, Song S Y, Choi S H and Park S Y 2008 *Appl. Phys. Lett.* **92** 023306
[18] Muller T and Nienhaus H 2003 *J. Appl. Phys.* **93** 924
[19] Koch R 1994 *J. Phys.: Condens. Matter* **6** 9519
[20] Bieganski P 2004 *Vacuum* **74** 211
[21] Haacke G 1976 *J. Appl. Phys.* **47** 4086
[22] Guillén C and Herrero J 2011 *Thin Solid Films* **520** 1
[23] Fanga Z B, Yan Z J, Tan Y S, Liu X Q and Wang Y Y 2005 *Appl. Surf. Sci.* **241** 303
[24] Lin T C, Chang S C and Chiu C F 2006 *Mater. Sci. Eng. B* **129** 39
[25] Song J O and Seong T Y 2004 *Appl. Phys. Lett.* **85** 6374
[26] Sahu D R and Huang J L 2006 *Appl. Surf. Sci.* **253** 827
[27] Sahu D R and Huang J L 2007 *Thin Solid Films* **516** 208
[28] Lee H M, Lee Y J, Kim I S, Kang M S, Heo S B, Kim Y S and Kim D 2012 *Vacuum* **86** 1494